Short Communication
Approach for using measured soil gas diffusion coefficients in Hydrus 1D with examples from forest soils

Christoph Haas[1]*, Sinikka Paulus[2,3], Martin Maier[3,4], Hubert Jochheim[5], and **Horst H. Gerke[1]**

[1] Working Group "Hydropedology", Research Area 1 "Landscape Functioning", Leibniz Centre for Agricultural Landscape Research (ZALF), Eberswalder Str. 84, 15374 Müncheberg, Germany
[2] Max Planck Institute for Biogeochemistry, Hans-Knöll-Straße 10, 07745 Jena, Germany
[3] University of Freiburg, Chair of Soil Ecology, Bertoldstraße 17, 79098 Freiburg, Germany
[4] Forest Research Institute Baden Württemberg (FVA), Wonnhaldestraße 4, 79100 Freiburg, Germany
[5] Working Group " Ecosystem Modelling", Research Platform "Models & Simulation", Leibniz Centre for Agricultural Landscape Research (ZALF), Eberswalder Str. 84, 15374 Müncheberg, Germany

Abstract

The use of Hydrus-1D for modeling soil gas fluxes can be improved by introducing a parameter *f* obtained by fitting the Millington–Quirk (MQ) tortuosity model to measured gas diffusion coefficients. The approach was tested for data from soil horizons of two sandy forest sites located in Northeast-Germany. *f*-values ranged between 0.41 and 0.54, indicating a more tortuous pore systems than predicted by MQ model (*f* = 1). The parameter optimization procedure can be carried out by using the statistical software R and the enclosed R-script.

Key words: forest soil / gas transport / Millington–Quirk / Pore tortuosity

Accepted August 14, 2020

Supporting Information available online

1 Introduction

Molecular diffusion is the main transport process responsible for gas exchange in soils (*Gliński* and *Stępniewski*, 1985) and is controlled by the gas concentration gradient [$\partial c/\partial x$, (mol m^{-4})]. This process is described by Fick's law in one-dimensional form as:

$$J = D_s \times \partial c/\partial x, \quad (1)$$

with the flux, J (mol m^{-2} s^{-1}), and the gas- and temperature-dependent effective diffusion coefficient of the soil, D_s (m^2 s^{-1}). One-chamber (*Flühler*, 1973) or double-chamber (*Rolston* and *Moldrup*, 2002) experiments are typically performed to determine D_s at the soil core-scale. Eq. (1) is used to calculate D_s under the assumption that all gas fluxes are solely caused by diffusion. However, D_s is heterogeneously distributed in soils at the micrometer-scale (*Haas* and *Horn*, 2018), the soil core-scale (*Moldrup* et al., 2001; *Haas* et al., 2019; *Mordhorst* et al., 2017, 2018), and at the soil profile scale (*Kühne* et al., 2012; *Maier* et al., 2017). The diffusion coefficient of, for example, oxygen in air is 10,000 times higher than in water (*Himmelblau*, 1964; *Gliński* and *Stępniewski*, 1985) and 1,000,000 times higher than in solid mineral (*Jost*, 1960). Since soils are three-phase systems (gaseous, liquid, and solid phase), the value of D_s strongly depends on the air-filled porosity and its continuity and connectivity.

The soil structure-related flow path lengths and the connectivity of the air-filled pore network is described by the tortuosity, τ, which can be derived from soil gas diffusivity measurements and estimated from diffusivity models. Tortuosity has frequently been described (*Šimůnek* et al., 2013) according to *Millington* and *Quirk* (1961), τ_{MQ}, as:

$$\tau_{MQ} = \theta_a^{7/3}\, \theta_s^{-2}, \quad (2)$$

with the air-filled porosity θ_a (m^3 m^{-3}) and the total porosity θ_s (m^3 m^{-3}). The MQ model [Eq. (2)] is expected to perform well for sandy soils (*Šimůnek* et al., 2013) since it was derived assuming randomly distributed solid particles of equal size. However, in natural soils (*e.g.*, agricultural or forest soils) the MQ model may not adequately fit to measured values of D_s.

Soil gas fluxes have been calculated using the gradient method (*Maier* and *Schack-Kirchner*, 2014). The Hydrus-1D program (*Šimůnek* et al., 2005) is widely used to numerically simulate the flow of water, gas, heat, and the transport of solutes in soils using the finite element method. Regarding simulations of carbon dioxide flues with Hydrus-1D, τ_{MQ}, is used to obtain D_s as:

$$D_s = D_0 \times \tau_{MQ}, \quad (3)$$

where D_0 is the molecular diffusion coefficient (*i.e.*, which is 1.59×10^{-5} m^2 s^{-1} for CO_2 in air. Thus, τ_{MQ} equals the relative diffusion coefficient D_s/D_0, which is often used to present

* Correspondence: C. Haas; e-mail: christoph.haas@zalf.de

measured D_s values, because it considers the impact of the specific measuring gas used.

We hypothesized that (1) by replacing τ_{MQ} in Eq. (3) with τ^*_{MQ}, defined as

$$\tau^*_{MQ} = \tau_{MQ} \times f, \quad (4)$$

where f is a fitting factor, D_s/D_0 can better be fitted to measured values as compared to Eq. (3). We further assume (2) that f can be derived from measured effective soil gas diffusivities determined with inert gases and (3) that f is a function of the soil type and depths.

It is the objective of this work to obtain f-values by fitting τ^*_{MQ} to measured values of D_s for soil data from two forest-sites. The horizon-specific f-values are qualitatively compared with soil structural observations and used to demonstrate how measured soil gas diffusion coefficients can be used in transport models that are using the MQ tortuosity model as in Hydrus-1D for example. The attached R-script, useable with the statistical software R (*R Development Core Team*, 2020), is constructed for a rapid determination of f-values using the Levenberg–Marquardt algorithm. Derived f-values can be used in Hydrus by replacing D_0 as input parameter by D^*_0 as derived by Eq. (5):

$$D^*_0 = f \times D_0. \quad (5)$$

2 Material and methods

Soil core samples (4.9 cm in height, 7.2 cm in diameter, 200 cm^3 in volume) were excavated from two forest sites: (1) a beech forest (*Fagus sylvatica* L.) site located in *Beerenbusch* (Brandenburg / Germany) and (2) a pine forest (*Pinus sylvestris* L.) site located in *Kienhorst* (Brandenburg / Germany). According to WRB, the soils are classified as Brunic Arenosol (Dystric) and Haplic Podzol at the beech and pine forest site, respectively. See Tab. 1 for details about the soil horizons and about the sand, silt, clay, soil organic carbon contents, and pH. At both sampling sites, six soil cores were excavated from the organic layers (O), five soil core samples were excavated from the topsoil [A(e)h and Ahe], and 15 samples were excavated from the subsoil horizons (Bhv and Bs). For the latter ones, sampling was carried out in increments of approximately 0.1 m (namely, L1 in 0.10–0.17 m, L2 in 0.18–0.25 m, L3 in 0.26–0.34 m), and five soil core samples were excavated from each layer.

The determination of the diffusion coefficient (D_s) of each soil core sample was repeated four times at different soil moisture levels, namely, (1) field fresh, (2) after a period of 24 h of air-drying, (3) after saturation by capillary rise, and (4) air-dried, aiming to reflect typical soil water contents (θ) of around 10–40 vol.-%. The actual values of θ and the air-filled porosity, θ_a, were calculated from the total porosity as determined by thermo-gravimetry after drying at 105°C for 24 h. The specific density of the solid soil material was determined by vacuum pycnometry (data not shown).

$D_{s,Ne}$ (*i.e.,* D_s for neon) of aggregated soil samples were determined with a one-chamber method (*Flühler*, 1973) with neon as tracer gas, which has a molecular diffusion coefficient in air of $D_{0,Ne} = 3.15 \times 10^{-5}$ $m^2 \times s^{-1}$ at T = 20°C and P = 101.33 kPa (*Fuller* et al., 1966). Soil cores (equipped with gaze at the bottom of the ring) were placed at the top of airtight cylinders in which neon was injected (*Kühne* et al., 2012). Decreasing Ne concentration in the chamber was measured over 45 min with a micro-gas chromatograph (CP2002P, Chrompack, Middelburg, Netherlands) and D_s was calculated as described in *Kühne* et al. (2012).

The statistical software R (*R Development Core Team*, 2020) and the R-implementation of the Levenberg–Marquardt algorithm (LMA) (*Elzhov* et al., 2016) were used for data processing and optimization. For details about the LMA see *Lourakis* (2005). By substituting τ_{MQ} with $\tau_{MQ}*$ [Eq. (4)] in Eq. (3) (with D_0 equal to $D_{0,Ne}$), the linear fitting parameter f, was derived with the LMA from measured values of D_s, air-filled, and total porosities by minimizing the sum of least-squares between modeled and measured values. The relative gas diffusion coefficient (D_s/D_0) linearly decreases or increases with changing f-values (Fig. 1). No differences in D_s/D_0 were visible close to water-saturation due to small values for D_s/D_0. However, D_s/D_0 is reduced by 20% (for $f = 0.8$) or increased by 20% (for $f = 1.2$) as compared to the situation without fitting ($f = 1$), *i.e.*, when the MQ model perfectly fits the measured values.

Thus, the LMA started assuming f to equal one. The fitting factor f can be used in Hydrus-1D simply by multiply $D_{0,CO2}$ with f.

Table 1: Soil horizons with corresponding depths, sand, silt, clay and organic carbon contents, and pH of the beech and pine forest sites.

	Horizon	Depth	Sand	Silt	Clay	SOC	pH
		(m)			($g\ kg^{-1}$)		
Beech	O	+0.05				191.8	4.9
	A(e)h	–0.07	880	91	29	37.8	5.0
	Bhv	–0.32	903	71	26	13.2	5.1
Pine	O	+0.05				257.1	3.6
	Ahe	–0.1	910	60	30	20.8	4.2
	Bs	–0.35	940	35	25	5.5	4.4

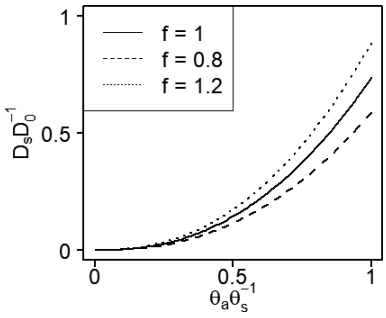

Figure 1: Relative soil gas diffusion coefficient (D_s/D_0) as a function of the relative air-filled pore space (*i.e.,* θ_a/θ_s) as calculated with the Millington–Quirk (MQ) model and as influenced by defined fitting factors *f* (namely *f* = 0.8; *f* = 1; *f* = 1.2); θ_s = 0.4.

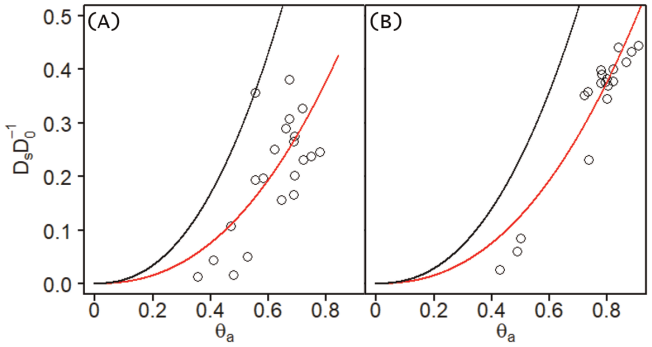

Figure 2: Relative diffusion coefficients (D_s/D_0) of the organic layers (O-horizons) of the beech site (A) and of the pine site (B) as a function of air-filled porosity (θ_a). The unfitted model is reflected by the black line, the fitted model [Eq. (4)] is presented by the red line. The number of considered data points, *n*, and the coefficient of determination, R^2, were 22 and 0.699 (beech), and 19 and 0.955 (pine), respectively.

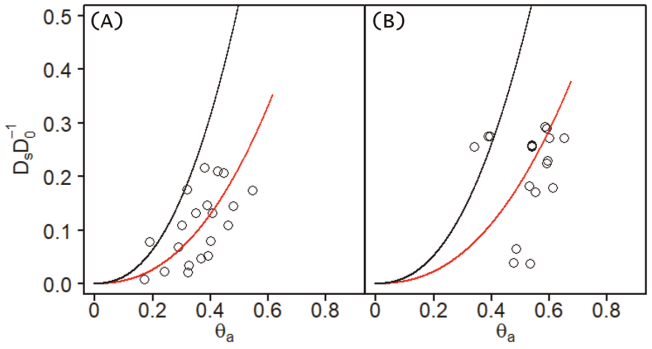

Figure 3: Relative diffusion coefficients (D_s/D_0) of the mineral topsoils (A-horizons) of the beech site (A) and of the pine site (B) as a function of air-filled porosity (θ_a). The unfitted model is reflected by the black line, the fitted model [Eq. (4)] is presented by the red line. The number of considered data points, *n*, and the coefficient of determination, R^2, were 20 and 0.623 (beech), and 18 and 0.433 (pine), respectively.

3 Results and discussion

For the organic layer of the beech forest (Fig. 2a), D_s was determined at evenly spread air-filled porosities values in the range of 0.36 to 0.78. At the pine site (Fig. 2b) data is nested (*i.e.*, some measurement points at low and some at high air-filled porosities). This is reasonable due to the considered moisture levels which ranged from water-saturated over field-fresh to air-dried. Water contents as determined for field-fresh samples were close to water contents of air-dried samples, reflecting the dry situation at the sampling site during the soil sampling campaign. For the mineral topsoil (A-horizon) at the pine site (Fig. 3b) measurement points with low air-filled porosities are missing. This indicates problems during the water-saturation process, which are potentially caused by hydrophobic substances reducing the wettability of soils (*e.g.*, *Haas* et al., 2018a) or by organic compounds that clog pores (*Hallett* et al., 2003). At all other horizons [namely A-horizon at the beech site (Fig. 3a) and both B-horizons (Fig. 4a, b)], data are homogeneously distributed, providing a valuable dataset for the evaluation of *f*. Air-filled porosities ranged from 0.36 to 0.91 for the organic layers to 0.14 to 0.65 for the mineral layers (*i.e.*, A and B horizons) (Tab. 2). Mean values of total porosities were highest for the organic layers (beech: 0.84; pine: 0.93) and decreased with increasing depths (Tab. 2).

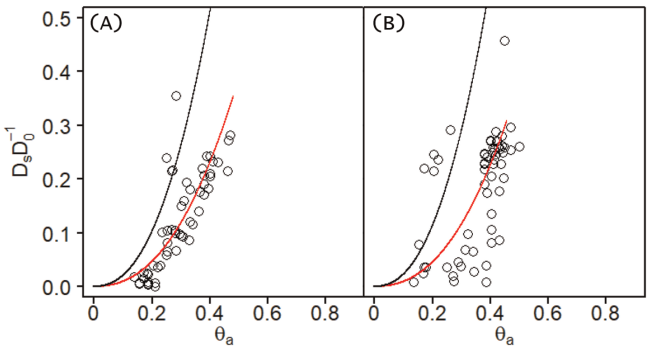

Figure 4: Relative diffusion coefficients (D_s/D_0) of the subsoil (B-horizon; L1, L2 and L3 were combined) of the beech site (A) and of the pine site (B) as a function of air-filled porosity (θ_a). The unfitted model is reflected by the black line, the fitted model [Eq. (4)] is presented by the red line. The number of considered data points, *n*, and the coefficient of determination, R^2, were 54 and 0.648 (beech), and 59 and 0.553 (pine), respectively.

For all horizons at both sites, *f* was significantly < 1 (Fig. 5) and ranged from 0.413 to 0.451 at the beech site and from 0.399 to 0.538 at the pine site (Tab. 2). That means, without fitting (*i.e., f* = 1), the MQ model significantly overestimates D_s. Fitting factors decreased with increasing soil depth at the pine site (Fig. 5) or were minimal at the mineral topsoil at the beech site. The confidence intervals (Fig. 5, Tab. 2), showed that the effective soil gas diffusivity of the organic layer at the pine site was significantly increased as compared to the organic layer at the beech site, reflecting very different physico-chemical (*e.g.*, wettability) and physical (*e.g.*, geometry) properties of the litter at both sites. More details about gas diffusion in forest humus layers can be found in *Maier* and *Lang* (2019). However, *f*-values (Tab. 2) indicated that the tortuosity of the pore systems at the two sampling sites was relatively variable and varied with soil depth (Fig. 5).

Table 2: Results for fitting parameter *f*. Mean values with lower and upper borders of the 95% confidence interval and degree of freedom, dF. Minimum $\theta_{a,min}$, maximal $\theta_{a,max}$ value and means of air-filled porosity, as well as means (with standard deviation) of total porosities (θ_s) of considered samples.

	Horizon	*f*	Conf (2.5%)	Conf (97.5%)	dF	$\theta_{a,min}$	$\theta_{a,max}$	$\theta_{a,mean(sd)}$	$\theta_{s,mean(sd)}$
Beech	O	0.449	0.396	0.503	21	0.36	0.78	0.62(0.11)	0.84(0.05)
	A(e)h	0.413	0.347	0.479	19	0.17	0.55	0.36(0.09)	0.62(0.07)
	Bhv	0.451	0.405	0.497	53	0.14	0.47	0.29(0.09)	0.48(0.04)
Pine	O	0.538	0.513	0.564	18	0.43	0.91	0.75(0.13)	0.93(0.03)
	Ahe	0.429	0.365	0.493	17	0.34	0.65	0.53(0.08)	0.68(0.11)
	Bs	0.399	0.362	0.437	58	0.14	0.50	0.36(0.09)	0.46(0.08)

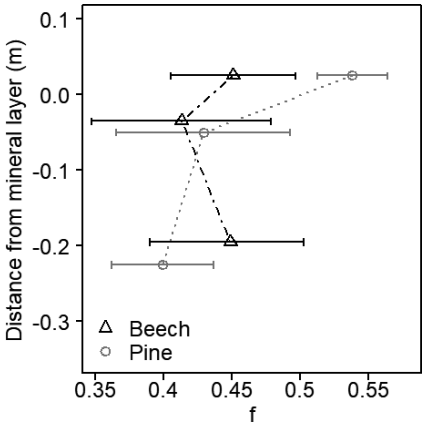

Figure 5: Means of fitting factor *f* (symbols) with 95%-confidence intervals (error bars) as a function of soil depths (here: mean depth of each soil horizon). See Tab. 2 for more details.

The *f*-values reflected the impact of the different pore systems, which depended on soil texture, organic carbon content and the distribution of the pore water that could be influenced by biological activity (*e.g.*, *Haas* et al., 2018b) or hydrophobicity (*e.g.*, *Haas* et al., 2018a) of the soils at the two sampling sites.

However, a more systematic investigation of the tortuosity and of *f*-values for better understanding differences in gas diffusion of soil pore systems was beyond the scope of the present study.

4 Conclusions

The study was carried out to test the use of *f*-values that are fitted from gas diffusion data for the application of the Millington–Quirk (MQ) tortuosity factor in numerical transport model such as HYDRUS-1D. Results for soil data of two forest sites suggested that the soil depths and site dependent *f*-values qualitatively reflected soil structural features. Future analyses of the *f*-values could be helpful for a better understanding of the influence of soil structure on gas transport processes.

While the standard MQ model represented mainly the upper range of observed D_s-values, the *f*-values that were < 1 reflected that in the soils of the two forest sites, the pore systems were more tortuous and less connected than predicted by the MQ model. The introduction of fitted *f*-values allowed the use of measured soil gas diffusion coefficients in models with the MQ tortuosity model. The fitting routine using Levenberg-Marquardt algorithm was programmed in a R-script (see appendix). The script provides a fast and reproducible procedure to determine horizon-specific *f*-values that can be used to manipulate input parameters for numerical simulations of, *e.g.*, carbon dioxide fluxes with Hydrus-1D. Further improvements in the understanding of the functioning of the tortuous pores in structured soils could be achieved by application of the methodology to data from differently-structured soils.

Acknowledgments

We thank the two anonymous reviewers for their valuable comments on our manuscript. This study was financially supported by the *Deutsche Forschungsgemeinschaft* (*DFG*), Bonn, in the framework of the *project GE 990/10-1*: "*Solute mass transfer through the macropore-matrix interface during preferential flow in structured soils: model development*" (*SOMATRA*).

Open access funding enabled and organized by Projekt DEAL.

Data Availability Statement

The data that support the findings of this study are available from the corresponding author upon reasonable request.

References

Elzhov, T. V., *Mullen, K. M.*, *Spiess, A.-N.*, *Bolker, B.* (2016): minpack.lm: R Interface to the Levenberg–Marquardt Nonlinear Least-Squares Algorithm Found in MINPACK, Plus Support for Bounds. R package version 1.2-1. Available at: https://CRAN.R-project.org/package=minpack.lm.

Fuller, E. N., *Schettler, P. D.*, *Giddings, J. C.* (1966): A new method for prediction of binary gas-phase diffusion coefficients. *Ind. Eng. Chem.* 58, 18–27.

Flühler, H. (1973): Sauerstoffdiffusion im Boden. *Mitt. Schweiz. Anstalt Forst. Versuchsw.* 49, 125–250.

Gliński, J., *Stępniewski, W.* (1985): Soil Aeration and Its Role for Plants. CRC Press, Boca Raton, FL, USA.

Haas, C., *Horn, R.* (2018): Impact of small-scaled differences in micro-aggregation on physico-chemical parameters of macroscopic biopore walls. *Front. Environ. Sci.* 6. DOI: https://doi.org/10.3389/fenvs.2018.00090.

Haas, C., *Gerke, H. H.*, *Ellerbrock, R. H.*, *Hallett, P. D.*, *Horn, R.* (2018a): Relating soil organic matter composition to soil water repellency for soil biopore surfaces different in history from two Bt horizons of a Haplic Luvisol. *Ecohydrology* 11. DOI: https://doi.org/10.1002/eco.1949.

Haas, C., *Holthusen, D.*, *Horn, R.* (2018b): Biological alteration of flow properties of soil samples from two Bt horizons of a Haplic Luvisol determined with rheometry. *Front. Environ. Sci.* 6. DOI: https://doi.org/10.3389/fenvs.2018.00110.

Haas, C., *Horn, R.*, *Gerke, H. H.*, *Dec, D.*, *Zúñiga, F.*, *Dörner, J.* (2019): Air permeability and diffusivity of an Andisol subsoil as influenced by pasture improvement strategies—Permeabilidad y diffusion de aire en el subsuelo de un Andisol sujeto a distintas estrategias de mejoramiento de praderas. *AgroSur J.* 46, 23–34.

Hallett, P. D., *Gordon, D. C.*, *Bengough, A. G.* (2003): Plant influence on rhizosphere hydraulic properties: direct measurements using a miniaturized infiltrometer. *New Pythol.* 157, 597–603.

Himmelblau, D. M. (1964): Diffusion of dissolved gases in liquids. *Chem. Rev.* 64, 527–550.

Jost, W. (1960): Diffusion in Solids, Liquids, Gases. Academic Press, New York, NY, USA.

Kühne, A., *Schack-Kirchner, H.*, *Hildebrand, E. E.* (2012): Gas diffusivity in soils compared to ideal isotropic porous media. *J. Plant Nutr. Soil Sci.* 175, 34–45.

Lourakis, M. I. (2005): A brief description of the Levenberg–Marquardt algorithm implemented by levmar. *Found. Res. Technol.* 4, 1–6.

Maier, M., *Longdoz, B.*, *Laemmel, T.*, *Schack-Kirchner, H.*, *Lang, F.* (2017): 2D profiles of CO_2, CH_4, N_2O and gas diffusivity in a well aerated soil: measurement and finite element modeling. *Agric. For. Meteorol.* 247, 21–33.

Maier, M., *Lang, V.* (2019): Gas diffusivity in the forest humus layer. *Soil Sci.* 184, 13–16.

Maier, M., *Schack-Kirchner, H.* (2014): Using the gradient method to determine soil gas flux: A review. *Agric. For. Meteorol.* 192, 78–95.

Millington, R. J., *Quirk, J. P.* (1961): Permeability of porous solids. *Trans. Faraday Soc.* 57, 1200–1207.

Moldrup, P., *Olesen, T.*, *Komatsu, T.*, *Schjønning, P.*, *Rolston, D. E.* (2001): Tortuosity, diffusivity, and permeability in the soil liquid and gaseous phases. *Soil Sci. Soc. Am. J.* 65, 613–623.

Mordhorst, A., *Zimmermann, I.*, *Fleige, H.*, *Horn, R.* (2017): Changes in soil aeration and soil respiration of simulated grave soils after quicklime application. *J. Plant Nutr. Soil Sci.* 180, 153–164.

Mordhorst, A., *Zimmermann, I.*, *Fleige, H.*, *Horn, R.* (2018): Improvement of oxygen transport functions in grave soils due to quicklime application depending on soil texture. *Geoderma* 331, 18–28.

R Development Core Team (2020): R: A Language and Environment for Statistical Computing. R Foundation for Statistical Computing, Vienna, Austria.

Rolston, E. R., *Moldrup, P.* (2002): Gas Diffusivity, in Dane, J. H., Topp, G. C. (eds.): Methods of Soil Analysis, Part 4, Physical Methods. SSSA, Madison, WI, USA, pp. 1113–1139.

Šimůnek, J., *Šejna, M.*, *van Genuchten, M. T.* (2005): The HYDRUS-1D Software Package for Simulating the One-Dimensional Movement of Water, Heat, and multiple solutes in Sariably-Saturated Media, Version 4.0x, Hydrus Series 1. Department of Environmental Sciences, University of California Riverside, Riverside, CA, USA.

Šimůnek, J., *Šejna, M.*, *Saito, H.*, *Sakai, M.*, *van Genuchten, M. T.* (2013): The HYDRUS-1D Software Package for Simulating the One-Dimensional Movement of Water, Heat, and Multiple Solutes in Variably-Saturated Media. Department of Environmental Sciences, University of California Riverside, Riverside, CA, USA.

